Evidence for *L*-dependence generated by channel coupling: ^{16}O scattering from ^{12}C at 115.9 MeV

Journal Item

Evidence for L-dependence generated by channel coupling: ^{16}O scattering from ^{12}C at 115.9 MeV

R. S. Mackintosh*

School of Physical Sciences, The Open University, Milton Keynes MK7 6AA, United Kingdom

(Received 27 April 2016; revised manuscript received 2 June 2016; published 6 September 2016)

Background: In earlier work, inversion of S matrix for 330 MeV ^{16}O on ^{12}C resulted in highly undulatory potentials; the S matrix resulted from the inclusion of strong coupling to states of projectile and target nuclei. L-independent S-matrix equivalent potentials for other explicitly L-dependent potentials have been found to be undulatory.

Purpose: To investigate the possible implications of the undulatory dynamic polarization potential for an underlying L dependence of the ^{16}O on ^{12}C optical potential.

Methods: S matrix to potential, $S_L \rightarrow V(r)$, inversion which yields local potentials that reproduce the elastic channel S matrix of coupled channel (CC) calculations, will be applied to the S matrix for 115.9 MeV ^{16}O on ^{12}C. Further, S_L for explicitly L-dependent potentials are inverted and the resulting L-independent potentials are characterized and compared with the undulatory potentials found for ^{16}O on ^{12}C.

Results: Some of the undulatory features exhibited by the potentials modified by channel coupling for 115.9 MeV ^{16}O on ^{12}C can be simulated by simple parameterized L-dependent potentials.

Conclusions: The elastic scattering of ^{16}O by ^{12}C is a particularly favorable case for revealing the effective L dependence of the potential modified by channel coupling. Nevertheless, there is no reason to suppose that undularity is not a generic property leading in many cases to the choice: nucleus-nucleus potentials are (i) smooth and L-dependent, (ii) L-independent and undulatory, or (iii) both.

DOI: 10.1103/PhysRevC.94.034602

I. INTRODUCTION

The possibility that L dependence might be a generic property of the nucleus-nucleus optical model potential (OMP) is unwelcome. It would obviously be inconvenient since standard direct reaction codes would require modification. This would not be straightforward since there is a great multiplicity of ways in which the OMP might be L dependent.

Nevertheless, the possibility that L dependence is a general property of the optical model potential should be considered. Arguments for the L dependence of OMPs for nucleons and some light ions have been presented in Ref. [1], a key point being the relationship between the undulatory ('waviness') and explicit L dependence of potentials. There exist cases of proton elastic scattering, see, e.g., Ref. [2] and others cited in Ref. [1], where precise model-independent, and L-independent, fitting of elastic scattering observables leads to undulatory potentials. Such undulations indicate an underlying L dependence. Such L dependence is predicted by formal reaction theory and explicit calculations [3–7]. Highly undulatory potentials have also been found with precision model-independent fitting of deuteron elastic scattering observables, see Refs. [8,9]. For heavier ions, there is very little elastic scattering data of sufficient precision and angular range to allow satisfactory model independent fitting. This is clear from a close examination of the fits in reviews such as Refs [10,11]. An exception is the case [12] of ^{16}O on ^{28}Si in which wide angular range data for several energies were fitted simultaneously, and undulations were indeed found. More generally, an obvious problem for identifying L dependence phenomenologically is the small differential cross section at backwards angles at high energies. Moreover a restricted angular range is imposed for pairs of identical bosons. One case where this does not apply, and where there is a high degree of nucleus-nucleus overlap, is ^{16}O on ^{12}C, and recent work involving this case presents a particular opportunity. In the course of explaining remarkable features in the elastic scattering angular distribution, Ohkubo and Hirabayashi [13] calculated the elastic scattering S-matrix S_L for 115.9 MeV ^{16}O. The excitation of strongly coupled cluster model states had a very strong effect on the elastic scattering angular distribution, modifying it and leading to an angular distribution that was very far from that of any standard folding model.

It is worth noting, following Refs. [3–5,7], that the dynamic polarization potentials (DPPs) arising from channel coupling are both L-dependent and dynamically nonlocal. It is difficult to separate the effects of these two properties, but it is likely that the L dependence is primarily responsible for the undulatory character of the local and L-independent equivalent potential. I therefore refer in what follows simply to L dependence, with the understanding that the coupling effects generate dynamical nonlocality as well. The most widely discussed form of nonlocality, that which is due to knock-on exchange and which is phenomenologically represented by the Perey Buck form [14], apparently gives rise to no substantial undularity, see Ref. [15]. This exchange nonlocality is quite distinct from, and additional to, dynamical nonlocality arising from channel coupling, as discussed in Ref. [7]. Other exchange processes also give rise to a particular form of L dependence, namely, parity dependence, see Ref. [16]. Reference [17] presents evidence that parity dependence might arise from coupling effects. However, exchange-induced effects play no role in what follows.

*raymond.mackintosh@open.ac.uk

In what follows, $S_L \rightarrow V(r)$ inversion is applied to the elastic scattering S-matrix S_L calculated by Ohkubo and Hirabayashi. This makes it possible to present a local and L-independent representation of the contribution to the effective nucleus-nucleus potential of their particular, strong, channel coupling. The specific channel coupling included by Ohkubo and Hirabayashi, involving strongly coupled excited states of both ^{16}O and ^{12}C, is both plausible and gives a good qualitative representation of remarkable features in the elastic scattering angular distribution. These features could not be explained by a folding model without channel coupling or by standard local potentials consistent with general systematics. From the resulting inverted potential, which has marked undulatory features, the case will be made that an alternative, and arguably preferable, representation of the interaction is L dependent.

The particular case presented here is just one example of how the relationship between the undulatory and L dependence properties of the phenomenological optical model potential can be related to the underlying reaction theory.

Section II briefly presents some definitions relating to the Iterative Perturbative (IP) method [18–22] for $S_L \rightarrow V(r)$ inversion. The various terms defined will be used in the discussion of the results of the calculations.

Section III presents and discusses the undulatory potentials found by inverting S_L of Ohkubo and Hirabayashi [13] for ^{16}O on ^{12}C at a laboratory energy of 115.9 MeV.

Motivated by the results of Sec. III, Sec. IV presents and discusses the L-independent potentials found by inverting S_L produced by potentials having a specific model L dependency. This affords the opportunity to compare certain features of the potentials found in this way with those presented in Sec. III. The model calculations involve the same nuclei and the same energy as those of Ref. [13]. The key comparison is between (i) the potentials found by inverting S_L calculated with channel coupling and (ii) the L-independent potentials that have the same S_L as potentials having a known L dependency.

Section V discusses the results, and also makes some comments as to why it appears to be possible to avoid the issue of L dependence in many cases of elastic scattering.

Section VI briefly summarizes the findings. Throughout this text, the partial wave angular momentum of spinless projectiles will be denoted by upper case L.

II. INVERSION CODE IMAGO: DEFINITIONS

Some definitions are presented here that will be used in the discussion of results from the $S_L \rightarrow V(r)$ inversion code IMAGO [23]:

IP,SRP The iterative-perturbative (IP) inversion method [18–22] starts the iterative inversion process with a starting reference potential (SRP).

IB, SVD At each iteration, amplitudes for the elements of the inversion basis (IB) are determined using singular value decomposition (SVD) matrix operations.

S-matrix distance, σ After a sequence of iterations, the current potential can be plotted by IMAGO and compared with the SRP. The fits to the S-matrix S_L and to the angular distribution can also be plotted. IMAGO will associate different lines on the graphs with values of the 'S-matrix distance' σ which is defined below in Eq. (1).

Target S-matrix, The 'target S matrix' is the input S matrix that is to be inverted.

The quantity σ is defined in terms of two sets of S-matrix elements (SMEs), the S_L^1 and S_L^2 as follows:

$$\sigma^2 = \sum_L \left| S_L^1 - S_L^2 \right|^2. \tag{1}$$

In most cases, S_L^1 will be the the target of the inversion and S_L^2 will be the the S matrix for the current stage of the inversion. Successful inversions often result in values of σ that are three orders of magnitude lower than that for S_L calculated from the SRP. (Note that all of the above can be generalized to spin-half inversion of S_{lj} determining an interaction with a spin-orbit term. Spin-1 inversion leading to a tensor interaction is also possible.) In order to achieve very low σ, IMAGO allows the lower limit on the singular values of the SVD linear system to be progressively lowered; initial high values of this limit are required to avoid divergence. For further discussion of $S_L \rightarrow V(r)$ inversion see Ref. [22].

Standard practice when inverting S_L with the code IMAGO is to compare results with different choices of IB, SRP, and other parameters in order to establish the uniqueness of the potential. In some cases, as discussed below, it becomes difficult to identify a unique potential.

III. THE POTENTIAL FOUND BY INVERSION

The elastic scattering of ^{16}O on ^{12}C at 115.9 MeV is very interesting for several reasons, just one of them being the remarkable correspondence with certain meteorological rainbows [13]. The coupling to states of both projectile and target nucleus specified in Ref. [13] greatly modifies the elastic scattering angular distribution see Fig. 1. The coupling leads to S_L for the elastic scattering channel that, when inverted, yield strongly undulatory ('wavy' or 'oscillatory') L-independent potentials. The first such L-independent potential to be presented, 'CC2potx', shown in Fig. 2, corresponds to a low value of S-matrix distance $\sigma = 0.43 \times 10^{-3}$. For such low values of σ, the angular distribution calculated with the inverted potential would be indistinguishable from the coupled channel (CC) angular distribution in a figure such as Fig. 1, for all angles. Note that for the SRP, $\sigma = 0.875$ so that the inversion process has reduced σ by more than three orders of magnitude. The SRP in this and most cases is the 'bare' elastic channel potential, and its S_L corresponds to the channel coupling being switched off. Therefore, the difference between the solid and dashed lines in Fig. 2 is a representation of the DPP that is due to the coupling.

There are three obvious questions: 1. What do these very strong undulatory features mean? 2. Are they realistically a possible property of a nucleus-nucleus single channel interaction potential? 3. Is the potential CC2potx a unique solutions to the inversion problem?

The answer to the third question is 'no', it is not a unique solution to the inversion problem as will be seen from the

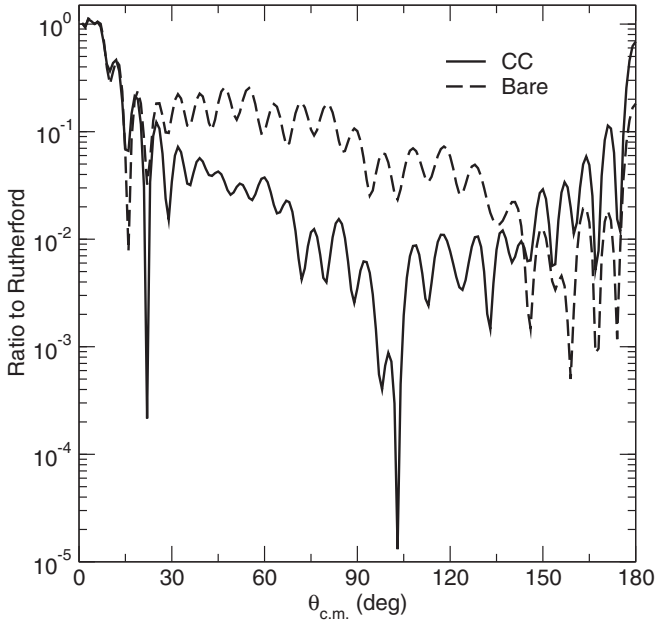

FIG. 1. Elastic scattering angular distributions for 116 MeV ^{16}O on ^{12}C. The dashed line is for scattering from the bare potential with no coupling. The solid line is for the full coupled channel calculation of Ref. [13].

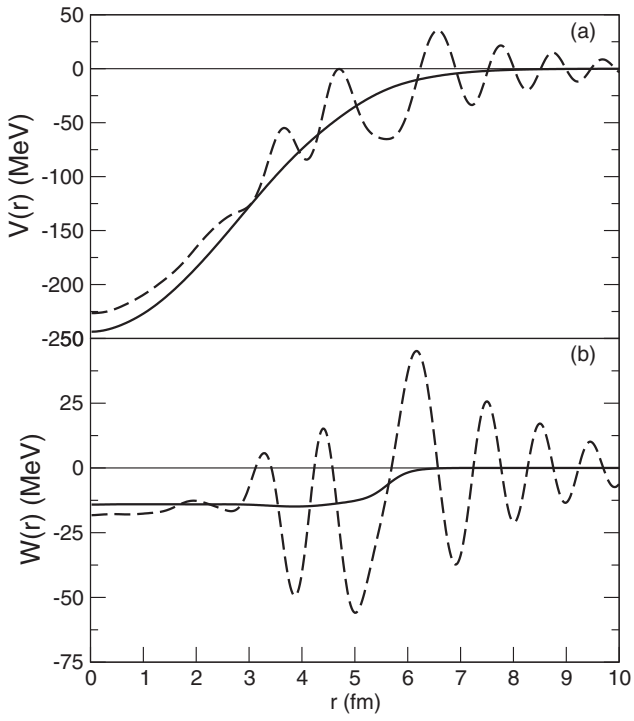

FIG. 2. The inverted potential CC2potx fitting S_L for 115.9 MeV ^{16}O scattering from ^{12}C, the real part is in (a) and the imaginary part in (b). The solid line is for the SRP which is the bare potential. The dashed line is for the inverted potential CC2potx with inversion $\sigma = 4.34 \times 10^{-4}$.

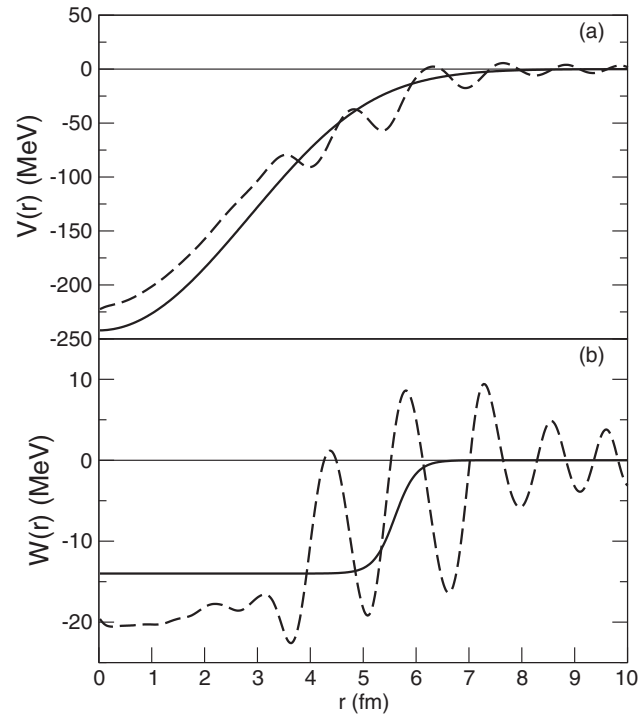

FIG. 3. The inverted potential CC3pot7 fitting S_L for 115.9 MeV ^{16}O scattering from ^{12}C, the real part is in (a) and the imaginary part is in (b). The solid line is for the SRP, the dashed line is for the inverted potential CC3pot7, $\sigma = 1.38 \times 10^{-4}$.

existence of alternative solutions in Figs. 3, 4 and 5. In cases where the S matrix corresponds to a reasonably smooth potential, IP inversion yields a practically unique solution. This can be established by comparing solutions with different SRPs, different IBs (IBs using different dimensionalities and sets of basis functions) and other parameters. This is usually straightforward, and spurious oscillations can be eliminated. However spurious oscillations are possible because of the existence of 'transparent potentials'. A transparent potential is an oscillatory potential that, when added to an existing potential, leads to very small (effectively zero) changes in the S matrix and hence the observables. These can be eliminated from IP inversion, except when the true potential that is sought is also highly oscillatory, in which case there is no natural 'smoothest' potential. That seems to be the case here. The problem is considerably less severe for ^{16}O on ^{12}C at higher energies, as in the 330 MeV case [24,25] where there is a larger number of partial waves to determine the potential. Moreover, coupling effects tend to become somewhat weaker at higher energies.

The answer to the second question is that strong undulations are indeed a property of a nucleus-nucleus interaction that includes the effect of strong inelastic couplings as in the present case.

Concerning the four solutions presented here: the imaginary part of CC2potx (Fig. 2) has extreme undulations which extend to a radius far beyond 10 fm. Potential CC3pot7 (Fig. 3) has much less extreme undulations in the imaginary part, but they also extend unrealistically far out. It was found that

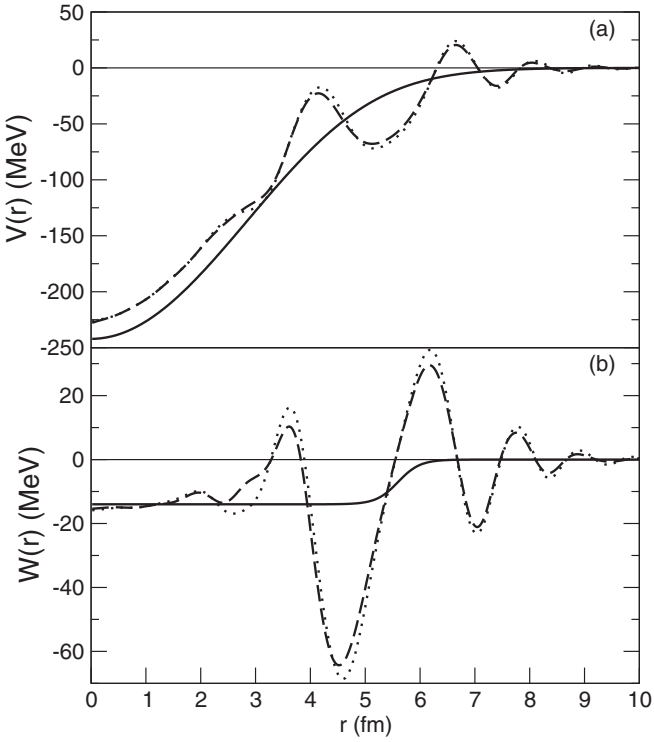

FIG. 4. The inverted potential CC4pot7 fitting S_L for 115.9 MeV ^{16}O scattering from ^{12}C, the real part is in (a) and the imaginary part is in (b). The solid line is for the SRP (the bare potential), the dotted line is for the inverted potential CC4pot7, $\sigma = 1.01 \times 10^{-3}$, and the dashed line is the potential for an earlier iteration, $\sigma = 1.55 \times 10^{-3}$.

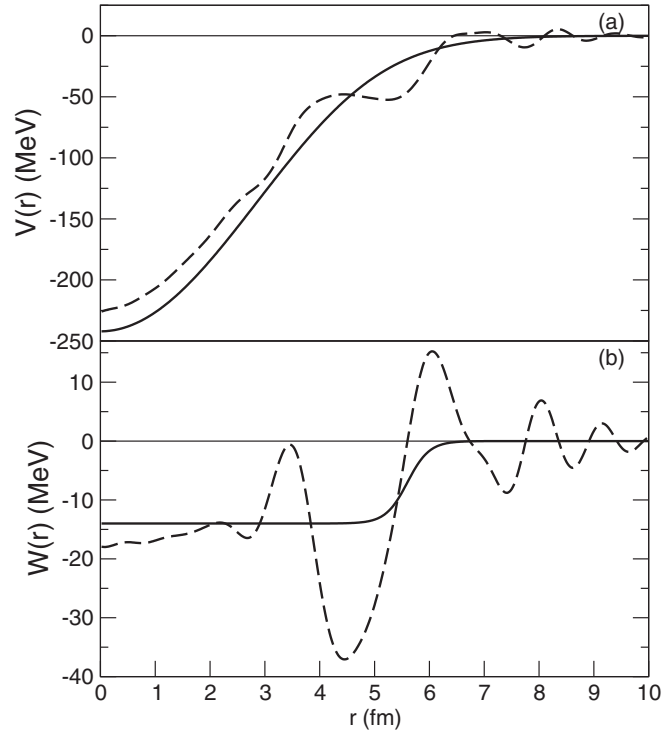

FIG. 5. The inverted potential CCXpot12 fitting S_L for 115.9 MeV ^{16}O scattering from ^{12}C, the real part is in (a) and the imaginary part is in (b). The solid line is the SRP (the bare potential) and the dashed line is the inverted potential, $\sigma = 1.03 \times 10^{-3}$. Note that the vertical scale for the imaginary part is different from that in Fig. 4.

solutions which do not extend to unrealistically large radii can be found as in CC4pot7 (Fig. 4, the dotted line), but apparently at the cost of large excursions in the imaginary part and a higher value of $\sigma = 1.01 \times 10^{-3}$, about 7 times higher than for CC3pot7. In general, following any sequence of iterations, the undulations increase as σ falls, and this can be seen in Fig. 4 where the dashed line represents the potential for an earlier iteration, with $\sigma = 1.55 \times 10^{-3}$. The tendency for the undularity to increase as σ falls is evident. An independent inversion (involving an alternative initial inversion basis) led to the potential CCXpot12, shown as the dashed line in Fig. 5, which has the same overall shape as potential in Fig. 4 and comparable inversion σ. The angular distribution corresponding to the CCXpot12 is graphically indistinguishable from the angular distribution for the CC calculation. For CCXpot12, the inversion $\sigma = 1.03 \times 10^{-3}$. The undulations of the potential in Fig. 5, while having the same general shape as those in Fig. 4, are of much smaller amplitude, noting the different scale for the imaginary term. The real components of the potentials in Figs. 4 and 5 have almost the same volume integral in spite of the different amplitude of the undulations, and both have a similar increase in rms radius compared to the bare potential. In fact, all of the potentials of Figs. 2–5 exhibit the same uniform repulsive effect for a radius of less than about 3 of 4 fm. For the imaginary components, the volume integrals and rms radii of the potentials in Figs. 4 and 5 are quite similar, and in both cases the volume integrals are greater and the rms radii are less than those of the bare potential. The potential CCXpot12 in Fig. 5 provides the provisional best potential representation of the elastic scattering S matrix from the CC calculations [13]. All the potentials presented in Figs. 2 through 5 yield angular distributions that are graphically indistinguishable out to 180° from the CC angular distributions on the scale of the figures.

Less undulatory potentials inevitably have higher inversion σ and fit a limited angular range. For example, a potential on the iterative path to CCXpot12 with σ a factor of 10 times larger had similar general features: the imaginary term had a dip at 4 fm and a peak at 6 fm although somewhat less pronounced. The angular distribution for this potential had clear differences from that for the CC calculation beyond ∼80°. These differences were typically a factor of 3 for many angles and a factor of 6 at 180°.

It is now clear that I have not provided a unique answer to the following basic question: what L-independent potential corresponds to the S matrix generated by the relevant channel coupling? However, it is quite certain that no non-undulatory, L-independent potential could ever give anything approaching a good fit to the angular distribution that is calculated from the S matrix generated by the coupled channel model of Ref. [13]. It is very reasonable to assume that the same would apply to the experimental data that the calculations of Ref. [13] approximately fit. A tentative answer to question 1 above can be given as follows: The strong undulations present an

alternative: either the potential for the case in question is indeed highly undulatory, or it is L dependent (it might be both). The question of how generic this alternative is must be the subject of further work; the question of why smooth and L-independent potentials are so often considered acceptable will be commented upon in Sec. V.

In the course of determining potentials that reproduce the CC S matrix, fits of a precision are required (and achieved) that are not approached in conventional phenomenology. However, there is a possible relevance to conventional phenomenology: the ambiguities, corresponding to transparent potentials, that have been found for 115.9 MeV ^{16}O scattering on ^{12}C, are likely to be present in model-independent fits (spline, sum of Gaussian, etc.) to precision experimental angular distribution data of wide angular range.

IV. MODEL L DEPENDENCE

In Ref. [1] some examples were given, for light ion cases, of the relationship between L-dependent potentials and the corresponding L-independent potentials with the same S_L or, in the case of nucleons the same S_{lj}. I now present a preliminary exploration of the relationship between L dependence and the corresponding undulatory nature of L-independent S-matrix-equivalent potentials. The examples all relate to the scattering of ^{16}O from ^{12}C at a laboratory energy of 115.9 MeV so as to maximize the relevance to the situation in Sec. III.

The idea is to take L-independent potentials, impose L dependence upon them and invert the resulting S matrix in order to study undulations that might arise in those L-independent potentials that are equivalent, in terms of S_L, to the L-dependent potentials. The initial L-independent potentials have simple Woods-Saxon forms. The real part is chosen to be roughly like the bare folded potential of Ref. [13] and the imaginary part is exactly the imaginary Woods-Saxon (WS) term given in that reference. The WS parameters for the real part are $V = 250$ MeV, $R = 3.0$ fm, and $a = 0.65$ fm and for the imaginary part $V = 14$ MeV, $R = 5.6$ fm, and $a = 0.3$ fm.

The imposed L dependence is simple and takes the form of added terms $v(r) \times f(L)$ or $w(r) \times f(L)$ where the $f(L)$ factor multiplying a real $[v(r)]$ or imaginary $[w(r)]$ terms is given by

$$f(L) = \frac{1}{1 + \exp\left((L^2 - \mathcal{L}^2)/\Delta^2\right)}. \tag{2}$$

In the present calculations, $v(r)$ and $w(r)$ each have a Woods-Saxon form with the same radius and diffusivity parameters as the corresponding real and imaginary L-independent terms. As a result, the L-dependent potentials essentially have a renormalized real or imaginary component for L less than $\mathcal{L}$, with a fairly sharp transition since Δ is quite small. The potential is unmodified for values of L substantially greater than $\mathcal{L}$. This pattern is motivated by the tendency for undulatory potentials to arise particularly when there is a substantial change for partial waves having L values around the point where $|S_L| \sim \frac{1}{2}$.

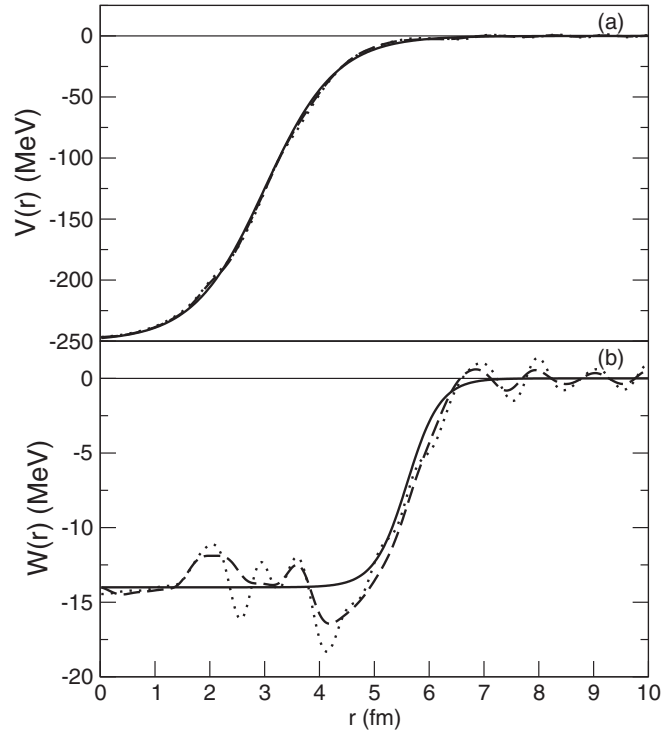

FIG. 6. The solid lines presents the real (a) and imaginary (b) parts of the L-independent potential. The dashed and dotted lines present inverted potentials, reproducing S_L calculated with an imaginary L-dependent term defined in the text. Two inverted potentials are presented, the dotted line with $\sigma = 0.378 \times 10^{-3}$ and the dashed lines, an earlier iteration with $\sigma = 0.523 \times 10^{-3}$.

A. Including an L-dependent imaginary part

The added L-dependent imaginary term is generated according to the above prescription as $w(r) \times f(L)$. The L-dependent factor $f(L)$, see Eq. (2), was chosen to have $\mathcal{L} = 20$ and $\Delta = 2$. The radial factor $w(r)$ is, as described above, of the same radial from as the L-independent term but with a depth of 0.7 MeV. The effect is to increase the depth, but not the radial shape, of the imaginary part from 14 MeV to 14.7 MeV, a 5% increase, for values of L less than 20, with a fairly sharp transition to zero change for higher L. For $L = \mathcal{L}$, $|S_L| \sim 0.35$.

The results of inverting S_L from this L-dependent potential is the L-independent potential shown in Fig. 6 where the SRP for the inversion is given by the solid line and this is the L-independent potential. In this figure the dotted line corresponds to inversion $\sigma = 0.378 \times 10^{-3}$ and the dashed line for an earlier iteration corresponds to inversion $\sigma = 0.523 \times 10^{-3}$. It will be seen that the potential has a characteristic oscillatory feature in the surface which has an amplitude much greater than the potential there. This is quite similar to the surface feature in the imaginary potential in Fig. 4. The volume integral of the imaginary term is, in each case, greater than that of the L-independent potential, by 8.56% for the dashed case and 8.24% for the better fitting dotted case. This is nearly twice the increase imposed on the potential for values of L less than 20. The change in the volume integral of the real

part is 100 times smaller, amounting to a ∼0.2% change. In this sense the L dependence in the imaginary component has induced a relatively small change in the real component. However, although the imposed undulations are small on the scale of the figure, the magnitude is comparable to that of the undulations in the imaginary component, but they have a nearly zero volume integral.

The two potentials shown follow the general tendency for the undulations to become enhanced in amplitude as σ becomes smaller as the iterations progress, i.e., as S_L for the L-independent potential determined by inversion more closely approaches S_L for the L-dependent potential. Local regions of emissivity in the surface undulations, do not lead to a breaking of the unitarity limit since the well-fitted S_L are calculated to have $|S_L| < 1$. It follows that such excursions into local emissivity are not an argument against the potentials that were shown in Fig. 4 which exhibit similar undulations in the surface. It has been found that local regions of emissivity are a very common feature of DPPs representing coupling effects in a wide range of nuclear scattering cases. They also occur in some model independent fits to elastic scattering [1].

Naturally, there is no reason to expect that the model L dependence that has been introduced is a realistic representation of the effects of strong channel coupling. However, it does show that L dependence appears to be necessary to reproduce the effects of strong coupling with a smooth potential. Probably quite a small degree of L dependence is enough.

B. Including an L-dependent real part

Similar calculations were performed including just an L-dependent real part for the same scattering case and with the same L-independent terms. Again, the parameter $\mathcal{L}$ was 20.

The real potential was first increased from 250 MeV to 251 MeV for L less than 20, with the same fairly sharp transition. This represents a small percentage change in the potential for low L, although in absolute magnitude it was comparable to the change in the imaginary part (note however that the radial extent of the real potential is rather less than that of the imaginary term). The inverted potential had no strong surface undulations, unlike the case with the imaginary L dependence. The real potential had two regions where the potential is increased in depth: near the origin and near the surface. The real volume integral is increased by 0.59%, which is not unreasonable in view of the fact that the potential was increased by 0.4% for the lowest 20 partial waves, which are those with substantial penetration. The volume integral of the imaginary potential fell by just 0.19%, the positive and negative excursions roughly canceling.

To obtain a more visual result, $v(r)$ was increased by a factor of 10 so that the real potential was 260 MeV deep for L less than ∼20 with the same fairly sharp transition, suggesting a roughly tenfold modification modification of the L-independent potential. The L-independent potential shown as a dotted line in Fig. 7, does indeed depart from the solid line following the same pattern enhanced in magnitude by that factor. The increase in depth of the real potential in the lowest radial range and also around $r = 5$ fm is clear. The change in the volume integral is a 5.61% increase. The change

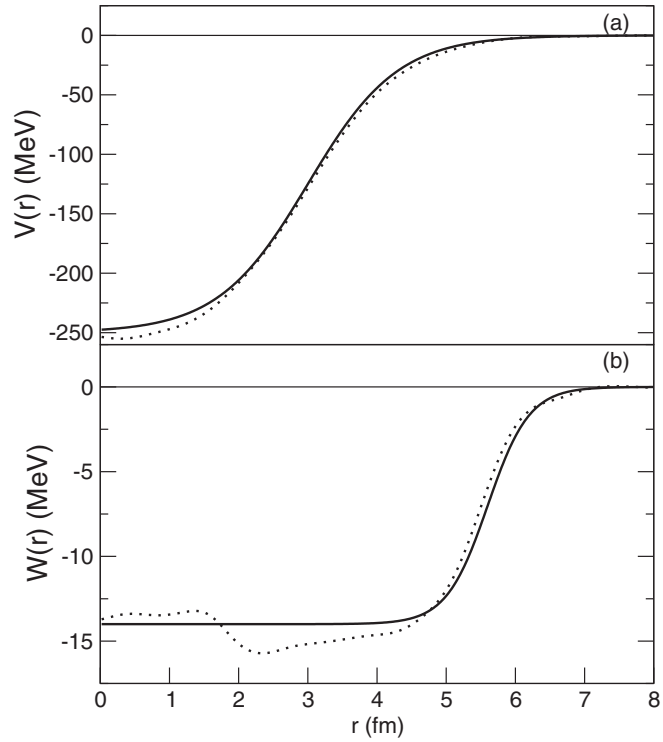

FIG. 7. Inversion of S_L from the enhanced (see text) L-dependent real term. The solid lines represent the real part (a) and imaginary part (b) of the SRP which is the unmodified the L-independent potential. The dotted lines represent the inverted potential with $\sigma = 0.799 \times 10^{-3}$.

in the imaginary part is qualitatively like that for the 1 MeV case, but much larger point-by-point. However the change in volume integral is very small indicating that the positive and negative changes cancel in the integration for $J_{\rm I}$. It appears to be a general rule that while a real L-dependent term leads to a perturbed real L-independent term having a substantial change in volume integral, the change in the imaginary term has a small volume integral although not small point by point. The converse is also true respecting an imaginary L-dependent term.

Because the unmodified real potential had a much smaller radial extent than the imaginary potential, that difference applied also to the added L-dependent term; this might relate to the absence of surface undulations in Fig. 7.

C. Larger radius L-dependent real part

It is possible that the relatively small amplitude of the undulations apparent in Fig. 7 is a result of the fact that the real potential, and so also the L-dependent change in the real potential, have a much small radial extent that the imaginary potential. The rms radius of the real potential is just 3.352 fm compared with 4.479 fm for the imaginary part. A further calculation was performed in which the L-dependent term was increased in radius, but with the same depth, leading to an rms radius of 3.929 fm. The L-dependent term is therefore no longer proportional to the L-independent term as in the previous cases.

The increase in radius of the L-dependent term increases the volume integral to 8.16% of the L-independent term. This can be compared to the 4% for the L-dependent term (i.e., corresponding to the 260 MeV depth for this term) that gave rise to the dotted lines in Fig. 7. With this new L dependence, the inverted potential exhibited undularities comparable in magnitude (and ambiguity) to those shown in Figs. 3 and 4. Plots (not shown) of arg S_L and $|S_L|$ reveal that whereas the previous L-dependent term, with the smaller radius, had no visible effect on S_L above L for which $|S_L| \sim 0.05$, the term with the larger radius visibly modified S_L for values of L for which $|S_L| \sim 0.5$. That corresponds to $L \sim 20$, i.e., the value of $\mathcal{L}$. This confirms that L-dependent effects lead to substantial undulations when there is a substantial difference in the effective potential for partial waves having L above and below the value for which $|S_L| \sim 0.5$.

D. Choice of L dependency

There are too many possible forms of L dependence for an exhaustive study here, but it has been shown that S_L from the CC calculations of Ref. [13] implies L dependence in both the real and imaginary potentials generated by the coupling. Other forms of L dependency have been applied to heavy ion interactions, and those forms that do not involve a distinct change between high and low partial wave, as in Eq. (2) when $\mathcal{L} \sim L_t$ with $|S_{L_t}| \sim 0.5$, may not lead to strong undulations.

An example of L dependence in the real part is provided by the RGM calculations of Wada and Horiuchi [26] for ^{16}O+^{16}O elastic scattering. The L dependence arises from exchange terms beyond the one-particle knock-on exchange that is normally included implicitly in folding models. Horiuchi [27] reviews such calculations in the context of a more general discussion of microscopic nucleus-nucleus potentials. The set of S_L values corresponding to the L-dependent real potentials of Wada and Horiuchi have been inverted [28] to yield an L-independent potential which is significantly different at lower energies from that derived [26] using WKB methods. The difference between the equivalent complete L-independent potential from the L-independent (nonexchange) part of the Ref. [26] potential is most marked in the nuclear interior. This work clearly established that exchange processes lead to an L dependence of nucleus-nucleus interactions (in addition to any parity-dependence.) The L dependence of Wada and Horiuchi apples to partial waves that would, in a more realistic calculation, be strongly absorbed. This makes their L dependence difficult to establish or disprove experimentally.

The model for ^{16}O+^{16}O scattering of Kondo *et al.* [29], included a phenomenological L-dependent real term inspired by the model of Wada and Horiuchi, together with an L-dependent imaginary term. The S_L for the potential with both terms L dependent was readily inverted [30] and the resulting real potential had a very similar shape and energy dependence to that found [28] for the Wada-Horiuchi potential.

The L dependence of the real part of the Kondo *et al.* [29] potential was of an overall factor $V_0 + V_1 L(L+1)$, i.e., a gradual L dependence unlike that in Eq. (2). This, by design, leads to a very similar energy dependence for the L-independent potential found by inverting the Wada and Horiuchi [26] S matrix. It seems that there is a systematic qualitative difference between the equivalent L-independent potentials found for these 'gradual' L dependencies and the sharper Fermi-form L dependencies which tend to generate much more undulatory equivalent potentials.

Unfortunately, a consistent calculation involving both the full antisymmetrization and full channel coupling would be very difficult. However, it does seem that the effects of antisymmetrization affect the potential at a small radius and might therefore be less relevant when the strong absorption of realistic calculations makes effects near the nuclear center less significant.

V. DISCUSSION

The coupled channel calculations of Ref. [13] have three important characteristics: (i) they were based on an established cluster model for the interacting nuclei, (ii) they explained an otherwise unexplained large angle feature of elastic scattering, and (iii) an L-independent potential that reproduces their angular distribution in a single channel calculation has strongly undulatory features. These features include emissive regions, particularly in the nuclear surface. Such effects are likely to elude approximate fits to experimental angular distribution data that is of limited angular range.

The calculations presented here lead to the following conclusion that applies at least to the scattering case of our example: in order to generate, *using a potential without undulations*, the S-matrix S_L that reproduces the effect of channel coupling, the potential must be L dependent. In other words, in some cases at least, the representation through a potential model of the effects of strong channel coupling presents a choice between a potential that is undulatory and L independent and one that is L dependent. The same alternative has previously been firmly established for nucleons scattering from ^{4}He and ^{16}O and other cases [22]. For cases such as that considered here, the range of possible L dependencies makes it difficult to pin down the specific form of the L dependence of the potential.

In the case of nucleon scattering, it has been shown that coupling to collective states of the target nucleus generates a DPP having substantial undulations [31]. Formal theory shows [3–7] that the DPP is both L dependent and nonlocal in a complicated way that is unlike exchange nonlocality. However there are separate lines of evidence for both L dependence and the appearance in empirical potentials of departures from the smooth forms of customary parameterized or folding model potentials [1,2]. For an example of an empirical deuteron potential showing wavy features, see Refs. [8,9]. Such undularity might arise from the coupling to breakup channels, see for example Refs. [32,33]. There is a need for more model independent precision fits to wide angular range elastic scattering data, like Ref. [8]. The concept of a 'good fit' is highly context dependent, but in the present context, 'precision fit' means $\chi^2/\mathrm{DF} \sim 1$.

The question arises: why has L dependence not been widely accepted? For the case of proton scattering, it is only when precise fits to wide angular range data are demanded that the need for either waviness or L dependence becomes evident. It

is also the case that for nucleon elastic scattering from target nuclei away from closed shells, angular distributions tend to be smoother and, as a result, have less power to discriminate between potentials. For the case of heavier ions, it becomes difficult to measure angular distributions over a wide angular range. The angular distribution fitted in Ref. [13] for ^{16}O on ^{12}C at a laboratory energy of 115.9 MeV extended out to about 140°. This angular range would obviously be impossible for identical bosons. For the case of ^{16}O on ^{16}O at 350 MeV, experimental uncertainties appear to become large at around 55°. It has to be conceded that potentials with no hint of undulations can fit this angular distribution with an imaginary term that is very close to that which corresponds to the static model Glauber potential [34]; it would be very interesting to know what would be found if more precise data of greater angular range were fitted. Indeed, it would seem *a priori* that the contribution found in ^{16}O on ^{12}C scattering at 115.9 MeV [13] due to the excitation of states of ^{16}O would also contribute to ^{16}O on ^{16}O scattering at a similar energy.

The present calculation raises, but throws little light on, an important general question: how does the supposed L dependence depend upon energy? There certainly were undulatory features in the DPPs that were found at 330 MeV [25], but less severe, and the DPPs were more uniquely determined. For proton scattering, the L dependence appears to fall with increasing energy [35] and this may well be a general property.

It is important to note that although the L-dependent potentials and their S-matrix equivalent potentials have identical radial wave function outside the nucleus, they may be far from identical in the nuclear overlap region. The S-matrix equivalent potentials may then give very different results when applied in DWBA calculations of direct reactions. This has long been known and studied for the nonlocality that is due to exchange, but much less is known concerning the effects on reactions of the L dependence and the dynamical nonlocality that arise from channel coupling. This is under study, and some results have been established for nucleon scattering see Ref. [7]. Very recently, the effects of nonlocality on direct reactions have been studied [36,37], and similar studies are required for the effects of L dependence.

VI. SUMMARY

The L-independent potentials that yield the same S_L as the strong channel coupling in the case of 115.9 MeV ^{16}O on ^{12}C elastic scattering, Ref. [13], exhibit strong undulations. This is firmly established although the exact nature of these undulations is hard to pin down definitively. An oscillatory potential in the surface region appears to be required and local excursions into emissivity do not necessarily lead to the breaking of the unitarity limit. Simple model L-dependent potentials lead to elastic scattering S-matrices S_L that, when inverted, yield undulatory L-independent potentials. The undulations exhibit some of the same features that are characteristic of the potentials generated by collective coupling, including the oscillations in the surface. There is therefore a nonexclusive alternative: the potential is undulatory or it is L dependent. I conjecture that this would be found to apply generally if serious model-independent fitting of suitable elastic scattering data were carried out systematically.

There are very many ways in which L dependence could be introduced into a phenomenological potential, and in Sec. IV the choice was restricted to a single form each for the real and imaginary terms separately. It was found that an L-dependent real part, proportional to the L-independent real part, generated some moderate waviness in both real and imaginary terms of the corresponding L-independent potential, but the volume integral of the imaginary part was almost unchanged. Conversely, an L-dependent imaginary term left the volume integral of the real part almost unchanged, although it was perturbed point by point. The L dependence in the imaginary part generated wide amplitude undulations in the corresponding L-independent term. The underlying L-independent potential, upon which the L dependency was based, had an imaginary term that extended much further in radius than the real term. This is the origin of the lesser tendency for the initial L dependence in the real part to generate large amplitude undulations. Subsequently, the radius of the real L-dependent term was increased to the extent that it influenced S_L for partial waves with L for which $|S_L| \sim 0.5$; this did generate large amplitude undulations. There are many aspects of elastic scattering phenomenology to be explored in a similar way.

ACKNOWLEDGMENTS

I am deeply indebted to Prof. S. Ohkubo and Prof. Y. Hirabayashi for supplying S-matrix elements and other numerical data, and also for very insightful comments. I am also very grateful to Nicholas Keeley for producing publishable figures, and also for many helpful discussions. I am also grateful to the anonymous referee whose suggestions improved the presentation of this work.

[1] R. S. Mackintosh, arXiv:1302.1097v4.
[2] R. Alarcon, J. Rapaport, and R. W. Finley, Nucl. Phys. A **462**, 413 (1987).
[3] H. Feshbach, Ann. Phys. (NY) **5**, 357 (1958); **19**, 287 (1962).
[4] G. R. Satchler, *Direct Nuclear Reactions* (Clarendon Press, Oxford, 1983).
[5] G. H. Rawitscher, Nucl. Phys. A **475**, 519 (1987).
[6] V. A. Madsen and F. Osterfeld, Phys. Rev. C **39**, 1215 (1989).
[7] N. Keeley and R. S. Mackintosh, Phys. Rev. C **90**, 044602 (2014).
[8] M. Ermer, H. Clement, P. Grabmayr, G. J. Wagner, L. Friedrich, and E. Huttel, Phys. Lett. B **188**, 17 (1987).
[9] M. Ermer, H. Clement, G. Holetzke, W. Kabitzke, G. Graw, R. Hertenberger, H. Kader, F. Merz, and P. Schiemenz, Nucl. Phys. A **533**, 71 (1991).
[10] M. E. Brandon and G. R. Satchler, Phys. Rep. **285**, 143 (1997).
[11] D. T Khoa, W. von Oertzen, H. G. Nohlen, and S. Ohkubo, J. Phys. G: Nucl. Part. Phys. **34**, R111 (2007)
[12] A. M. Kobos, G. R. Satchler, and R. S. Mackintosh, Nucl. Phys. A **395**, 248 (1983).

[13] S. Ohkubo and Y. Hirabayashi, Phys. Rev. C **89**, 061601(R) (2014).
[14] F. G. Perey and B. Buck, Nucl. Phys. **32**, 353 (1962).
[15] R. S. Mackintosh and S. G. Cooper, J. Phys. G: Nucl. Part. Phys. **23**, 565 (1997).
[16] S. G. Cooper and R. S. Mackintosh, Phys. Rev. C **54**, 3133 (1996).
[17] G. H Rawitscher and D. Lukaszek, Phys. Rev. C **69**, 044608 (2004).
[18] R. S. Mackintosh and A. M. Kobos, Phys. Lett. B **116**, 95 (1982).
[19] S. G. Cooper and R. S. Mackintosh, Inverse Problems **5**, 707 (1989).
[20] V. I. Kukulin and R. S. Mackintosh, J. Phys. G: Nucl. Part. Phys. **30**, R1 (2004).
[21] R. S. Mackintosh, arXiv:1205.0468.
[22] R. S. Mackintosh, Scholarpedia **7**, 12032 (2012).
[23] S. G. Cooper, notes for IMAGO users, Open University report (unpublished) (1999).
[24] S. Ohkubo and Y. Hirabayashi, Phys. Rev. C **89**, 051601(R) (2014).
[25] R. S. Mackintosh, Y. Hirabayashi, and S. Ohkubo, Phys. Rev. C **91**, 024616 (2015).
[26] T. Wada and H. Horiuchi, Prog. Theor. Phys. **80**, 488 (1988); **80**, 502 (1988).
[27] H. Horiuchi, in *International Conference on Clustering Aspects of Nuclear Structure and Nuclear Reactions, Chester*, edited by J. S. Lilley and M. A. Nagarajan (Reidel, Dordrecht, 1984), p. 35.
[28] S. Ait-Tahar, R. S. Mackintosh, S. G. Cooper, and T. Wada, Nucl. Phys. A **562**, 101 (1993).
[29] Y. Kondo, B. A. Robson, and R. Smith, Phys. Lett. B **227**, 310 (1989).
[30] S. Ait-Tahar, S. G. Cooper, and R. S. Mackintosh, Nucl. Phys. A **542**, 499 (1992).
[31] R. S. Mackintosh and N. Keeley, Phys. Rev. C **90**, 044601 (2014).
[32] R. C. Johnson and P. Tandy, Nucl. Phys. A **235**, 56 (1974)
[33] R. S. Mackintosh and D. Y. Pang, Phys. Rev. C **86**, 047602 (2012).
[34] S. G. Cooper and R. S. Mackintosh, Nucl. Phys. A **576**, 308 (1994).
[35] A. M. Kobos and R. S. Mackintosh, J. Phys. G: Nucl. Phys. **5**, 97 (1979).
[36] L. J. Titus, F. M. Nunes, and G. Potel, Phys. Rev. C **93**, 014604 (2016).
[37] A. Ross, L. J. Titus, and F. M. Nunes, Phys. Rev. C **94**, 014607 (2016).